JID Open

# Exons 5–15 of Kazrin Are Dispensable for Murine Epidermal Morphogenesis and Homeostasis

Mariya K. Chhatriwala[1,5], Sara Cipolat[2,5], Lisa M. Sevilla[3], Rachida Nachat[4] and Fiona M. Watt[1,2]

Kazrin binds to periplakin and ARVCF catenin, and regulates adhesion and differentiation of cultured human keratinocytes. To explore kazrin function *in vivo*, we generated a kazrin gene-trap mouse in which only exons 1–4 were expressed, fused to β-galactosidase. On transient transfection, the protein encoded by exons 1–4 did not enter the nucleus, but did cause keratinocyte shape changes. The mice had no obvious defects in skin development or homeostasis, and periplakin and desmoplakin localization was normal. Expression of the kazrin-β-galactosidase fusion protein faithfully reported endogenous kazrin expression. Kazrin was not expressed in embryonic epidermis and was first detected at postnatal day 1. In adult mice, epidermal kazrin expression was less widespread than in humans and *Xenopus*, being confined to the bulb of anagen hair follicles, the infundibulum, and parakeratotic tail epidermis. In anagen bulbs, kazrin was expressed by a band of cells with elongated morphology and low desmoplakin levels, suggesting a role in morphogenetic cell movements. We conclude that exons 5–15 of kazrin, encoding the nuclear localization signal and C-terminal domain, are not required for epidermal development and function. The previously reported role of kazrin in regulating cell shape appears to reside within the N-terminal coiled-coil domain encoded by exons 1–4.

*Journal of Investigative Dermatology* (2012) **132,** 1977–1987; doi:10.1038/jid.2012.110; published online 19 April 2012

## INTRODUCTION

Kazrin is an evolutionarily conserved cytoplasmic and nuclear protein that was originally identified as a binding partner of periplakin, a component of epidermal desmosomes and the cornified envelope (Groot *et al.*, 2004). Five isoforms of kazrin have been described. The four short isoforms encode three proteins (kazrinA, B, and C/D) that have different N termini, but all contain a coiled-coiled domain responsible for binding periplakin, and a putative nuclear localization signal (NLS) (Groot *et al.*, 2004; Wang *et al.*, 2009). The short isoforms of kazrin have no known homologs. The long isoform, kazrinE, possesses additional 3′ exons that encode a C-terminal liprin homology domain that can associate with the leukocyte common antigen–related protein tyrosine phosphatase (Nachat *et al.*, 2009).

Overexpression of kazrinA stimulates terminal differentiation of cultured human keratinocytes and is associated with a reduction in F-actin content, disruption of desmosome assembly, and changes in cell shape. Overexpression of activated RhoA rescues the effects on cell shape and adhesion. Conversely, knockdown of kazrinA impairs terminal differentiation, but does so independently of RhoA activity (Sevilla *et al.*, 2008a). Overexpression of kazrinE also results in terminal differentiation of human keratinocytes and changes in cell shape. In addition, kazrinE colocalizes with stabilized microtubules in differentiating keratinocytes (Nachat *et al.*, 2009). All kazrin isoforms can form complexes with one another (Nachat *et al.*, 2009), raising the possibility that, together with periplakin and envoplakin, kazrin forms a cortical scaffold that integrates the actin cytoskeleton with desmosomes (Ruhrberg *et al.*, 1997; Kalinin *et al.*, 2001; Groot *et al.*, 2004).

Studies of kazrin function *in vivo* have been limited to *Xenopus* embryos, where depletion of endogenous kazrin results in striking defects in axial elongation, muscle and notochord differentiation, and epidermal morphogenesis. These effects are believed to be due to the disruption in the formation of cell–cell junctions (Sevilla *et al.*, 2008b; Cho *et al.*, 2010). Given the effects of modulating kazrin levels in cultured keratinocytes and in *Xenopus* embryos, we hypothesized that knocking out kazrin in mice would result in a severe epidermal phenotype. In this study, we have examined the phenotype of two independent lines of mice in which only the first four exons of kazrin are expressed.

[1]*Wellcome Trust Centre for Stem Cell Research, Cambridge University, Cambridge, UK;* [2]*CRUK Cambridge Research Institute, Li Ka Shing Centre, Cambridge, UK;* [3]*Instituto de Biomedicina de Valencia, CSIC, Valencia, Spain and* [4]*EA4233, UFR de Pharmacie, Clermont-Ferrand, France*

[5]*These authors contributed equally to this work.*

*Correspondence: Fiona M. Watt, Wellcome Trust Centre for Stem Cell Research, Cambridge University, Tennis Court Road, Cambridge CB2 1QR, UK. E-mail: fiona.watt@cancer.org.uk*

*Abbreviations: β-geo, β-galactosidase fused to a neomycin resistance gene; ES, embryonic stem; flx, conditional knockout; GST, glutathione-S-transferase; gt, gene trap; IFE, interfollicular epidermis; NLS, nuclear localization signal; P1, postnatal day 1; PBS, phosphate-buffered saline; siRNA, small interfering RNA; wt, wild type*

*Received 9 August 2011; revised 23 February 2012; accepted 1 March 2012; published online 19 April 2012*

## RESULTS

### Generation of mice lacking exons 5–15 of kazrin

Two different strategies were used to knock out kazrin, which made use of targeted embryonic stem (ES) cells available via SIGTR. In the first strategy, a gene trap consisting of β-galactosidase fused to a neomycin resistance gene (*β-geo*) was inserted between exons 4 and 5 of the murine kazrin gene (Figure 1a). Mice homozygous for the gene trap (gt/gt) expressed exons 1–4 of kazrin fused to β-geo (Figure 1b) instead of wild-type (wt) kazrin. To confirm that any observed

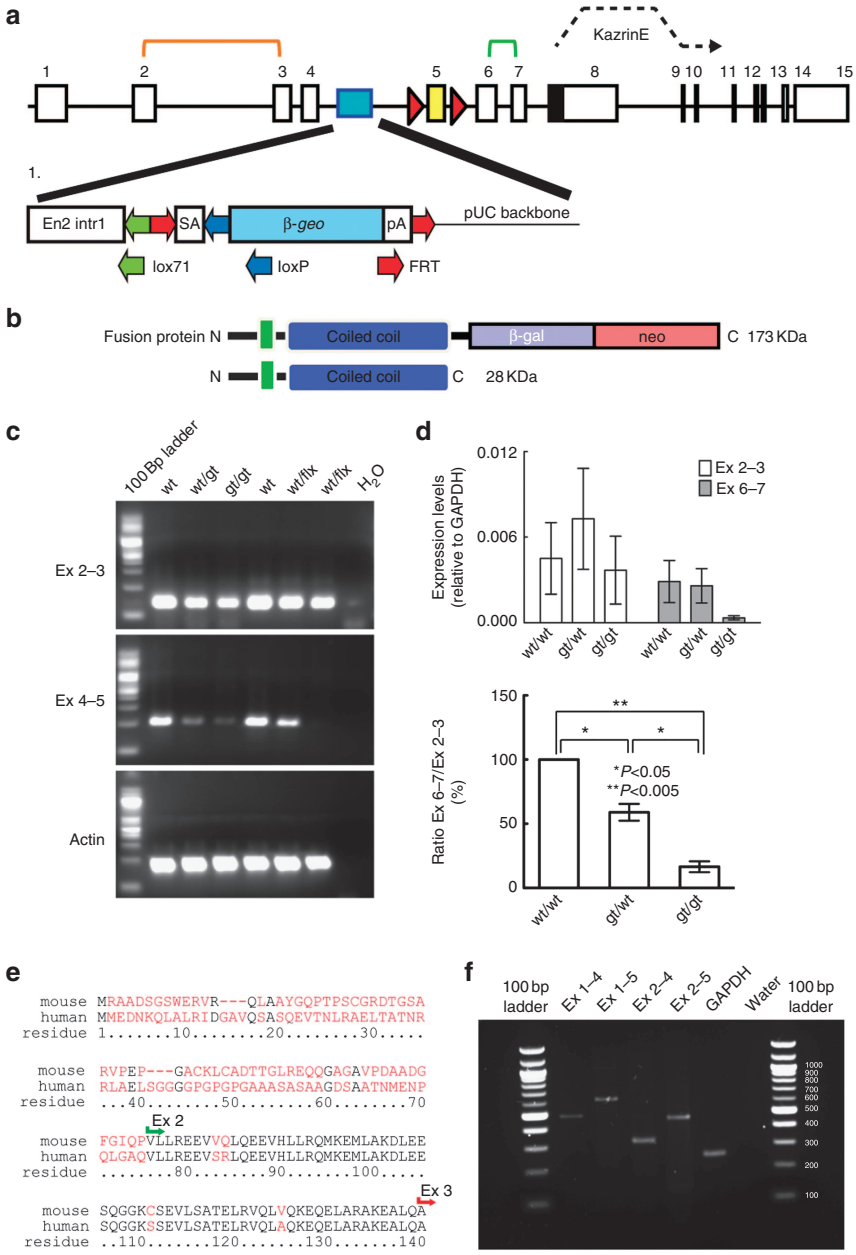


**Figure 1. Generation of kazrin β-galactosidase (β-gal) gene-trap (gt/gt) mouse and conditional knockout (flx/flx) mice.** (**a**) Exon structure of mouse kazrin. Blue box represents insertion of the neomycin resistance gene (*β-geo*) cassette in the kazrin β-gal gt/gt mouse. Red triangles indicate loxP sites for removing exon 5 in the kazrin flx/flx mice. (**b**) Predicted domain architecture of kazrin-β-geo fusion protein in the kazrin β-gal (top) gt/gt mouse and kazrin fragment expressed in the (bottom) kazrin flx/flx mouse. (**c**) RT-PCR amplification of transcripts upstream (exons 2–3) or downstream (exons 4–5) of the gene trap. RNA in each lane is from a single representative litter-matched mouse of the genotype indicated. (**d**) Quantitative RT-PCR of transcripts upstream (exons 2–3) and downstream (exons 6–7) of the gene trap. Top: Expression values relative to glyceraldehyde 3-phosphate dehydrogenase (GAPDH). Each bar shows the mean and standard deviation of at least three mice per genotype. Bottom: Ratio (%) of upstream and downstream transcripts from the top panel. Primer positions upstream and downstream of the *β-geo* cassette are indicated by the orange and green brackets, respectively, in **a**. (**e**) Alignment of predicted amino-acid sequences encoded by exons 1 and 2 of human kazrinA and mouse kazrin. (**f**) RT-PCR amplification of exons 1–4, 1–5, 2–4, or 2–5 of mouse kazrinA. Positive (GAPDH) and negative (water) controls are shown. *β-geo*, β-galactosidase fused to a neomycin resistance gene; Ex, exon.

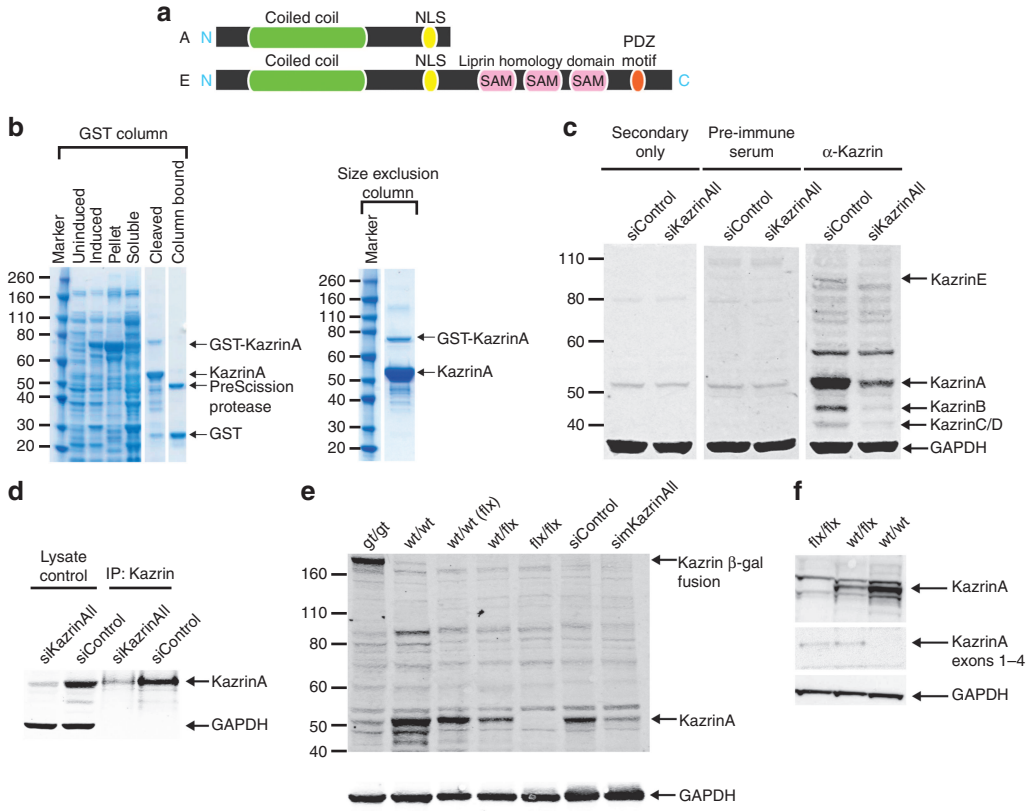


**Figure 2. Analysis of kazrin protein expression.** (**a**) Domain architecture of kazrinA and kazrinE. The N terminus of kazrinE is identical to kazrinA. (**b**) Purification of recombinant human kazrinA overexpressed in *Escherichia coli* as a glutathione-*S*-transferase (GST) fusion protein. (**c**) Lysates of normal human keratinocytes transfected with scrambled small interfering RNA (siControl) or pooled siRNAs specific for all isoforms of kazrin (siKazrinAll) were blotted with pan-kazrin antibody, rabbit pre-immune serum, or rabbit secondary antibody alone. (**d**) Pan-kazrin antibody crosslinked to protein G agarose beads was used to immunoprecipitate endogenous kazrin from lysates of normal human keratinocytes. (**e**, **f**) Pan-kazrin antibody detection of endogenous kazrin, kazrin β-galactosidase (β-gal) fusion protein, and the 28-kDa fragment encoded by kazrin exons 1–4 in lysates of wild-type (wt) mice or litter-matched gene trap (gt/gt) and conditional knockout (flx/flx) mice. simKazrinAll: wt/wt keratinocytes transfected with two pooled siRNAs (see also Supplementary Figure S1c online). Glyceraldehyde 3-phosphate dehydrogenase (GAPDH) was used as a loading control for **c**–**f**.

phenotypic effects were due to deletion of exons 5–15 and not due to the expression of the *β-geo* cassette, we used a second strategy whereby exon 5 of kazrin was flanked by loxP sites. Mice with the targeted gene were crossed with PGK-Cre mice; as a result, only exons 1–4 of kazrin were expressed (conditional knockout, flx/flx) in all tissues (Figure 1b). The gt/gt and flx/flx mice were born in normal Mendelian ratios, were fertile, and did not show any gross phenotypic abnormalities.

To confirm targeting of kazrin, we amplified kazrin mRNA using primers designed to amplify exons 2–3, 4–5, or 6–7 (Figure 1a, c, and d). Exons 2–3 were expressed at similar levels in wt, gt/gt, and flx/flx mice, as well as in heterozygous animals (wt/gt, wt/flx), when assessed by semiquantitative RT-PCR (Figure 1c) or quantitative RT-PCR (Figure 1d). In contrast, the levels of exons 4–5 (Figure 1c) and 6–7 (Figure 1d) were reduced in heterozygous mice and virtually undetectable in homozygous mice.

A comparison of the predicted protein sequences of human and mouse kazrin (as published on the USCS Genome Browser; http://genome.ucsc.edu/) revealed that the proteins encoded by exons 2–8 of mouse (accession number NP_001103155.1) and human (accession number NP_056024.1) kazrinA are over 90% identical, but there is significant divergence in exon 1 (Figure 1e). In contrast, exon 1 of mouse kazrinE is predicted to be identical to human kazrinA exon 1 (Okazaki *et al.*, 2004; Diez-Roux *et al.*, 2011). By using primers specific for exon 5 and for each predicted form of mouse exon 1 in mouse skin, we were able to amplify a kazrin fragment with the primer to the divergent exon 1 (Figure 1e), but not to the homolog of human kazrinA exon 1 (Figure 1f and data not shown). By using primer pairs for mouse exons 1 and 4, 2 and 4, 1 and 5, or 2 and 5, we amplified a single band (Figure 1f). Therefore, we did not obtain evidence for alternative splicing between exons 1 and 5 of mouse kazrin.

### Generation of antibodies to recombinant kazrin

The antibodies we previously generated to kazrin were raised against peptides corresponding to different domains and splice variants of the protein (Groot *et al.*, 2004; Sevilla *et al.*, 2008a; Nachat *et al.*, 2009). To generate a pan-kazrin antibody and maximize the number of binding sites available for antibody recognition, we overexpressed full-length

human kazrinA as a glutathione-*S*-transferase (GST) fusion protein in *Escherichia coli*. The GST tag was cleaved after the initial purification. KazrinA was further purified over a size-exclusion column before being used to immunize rabbits (Figure 2a and b). KazrinA has a predicted molecular mass of 47 kDa, but runs approximately 5–6 kDa higher on polyacrylamide gels (Groot *et al.*, 2004; Sevilla *et al.*, 2008a; Nachat *et al.*, 2009) (Figure 2b).

To determine whether the new antibody recognized endogenous kazrin, we immunoblotted lysates of primary human keratinocytes that had been transfected with either control small interfering RNA (siRNA) or a siRNA to all isoforms of kazrin (Figure 2c and Supplementary Figure S1a online). The antibody recognized bands with molecular masses corresponding to kazrin isoforms A, B, C/D, and E, which were reduced in abundance by kazrin siRNA transfection. The antibody also immunoprecipitated kazrin from lysates of primary human keratinocytes (Figure 2d). The kazrinA band detected with the antibody to recombinant kazrin had the same mobility as that detected with a commercial kazrin antibody and the pan-kazrin LS7 antibody we described previously (Sevilla *et al.*, 2008a; Supplementary Figure S1b online).

To test whether the new pan-kazrin antibody recognized mouse kazrin, we performed immunoblotting on lysates of keratinocytes cultured from wt/wt, gt/gt, wt/flx, and flx/flx mice, as well as wt/wt keratinocytes in which kazrin had been knocked down (Figure 2e and Supplementary Figure S1c and d online). The antibody recognized a band of approximately 180 kDa, corresponding to the kazrin β-galactosidase fusion protein in gt/gt cells, and detected endogenous short kazrin isoforms in wt/wt mice. In human keratinocytes, kazrinE is considerably less abundant than kazrinA (Figure 2c), and in mouse keratinocytes kazrinE protein was undetectable (Figure 2e). Lysates of primary keratinocytes cultured from adult kazrin flx/flx mice had no detectable full-length kazrin; however, on long exposures of the blots, a 28-kDa band, predicted to correspond to kazrin exons 1–4, was present in flx/flx and wt/flx cells, but not in wt/wt cells (Figure 2f).

We conclude that the antiserum generated against recombinant human kazrin detects all human kazrin isoforms and crossreacts with mouse kazrin. By probing blots of keratinocytes from the gt/gt and flx/flx mice, we confirmed successful deletion of full-length kazrin and expression of the N-terminal region encoded by exons 1–4, either as a β-galactosidase fusion protein (Figure 2e) or as a 28-kDa fragment (Figure 2f).

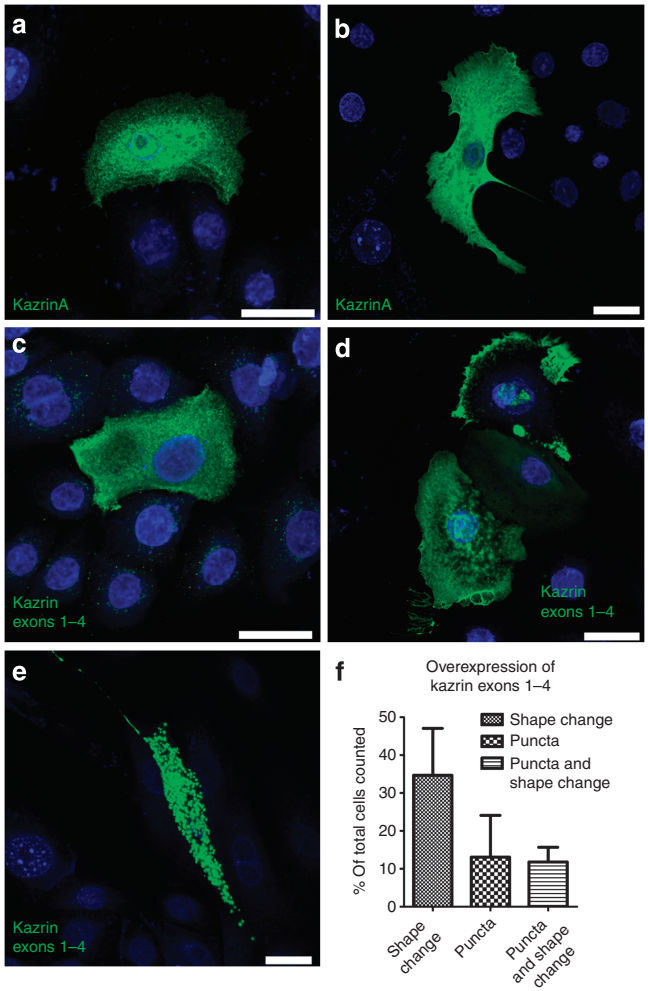


**Figure 3. Transient expression of full-length kazrin or exons 1–4 in cultured human keratinocytes.** (**a**–**e**) Immunolabeling of kazrin (green) with 4′,6-diamidino-2-phenylindole (DAPI) nuclear counterstain (blue). (**f**) Quantification of effect of kazrin exons 1–4 on cell morphology. Cells were scored as having altered cell shape (elongation/prominent filopodia/prominent lamellipodia), cytoplasmic kazrin puncta, or both. Data are mean ± SEM of three experiments. The numbers of cells scored per experiment were 128, 245, or 180. Bars = 25 μm. Ex, exon.

### Functional analysis of kazrin exons 1–4

Several studies have shown that full-length kazrin can localize to the nucleus in the epidermis and cultured cells (Groot *et al.*, 2004; Sevilla *et al.*, 2008a; Cho *et al.*, 2010), and mutation of key lysine residues in the NLS of *Xenopus* kazrin prevents nuclear accumulation (Cho *et al.*, 2010). The fragment of kazrin expressed in the gt/gt and flx/flx mice (exons 1–4) encompasses the majority of the coiled-coil domain, but lacks the NLS (Figures 1a and 2a).

To determine whether the protein encoded by exons 1–4 could nevertheless enter the nucleus, and whether or not it induced cell shape changes, a plasmid encoding exons 1–4

**Figure 4. Comparison of skin of wild-type (wt/wt) and kazrin gene trap (gt/gt) and conditional knockout (flx/flx) mice.** Sections of adult back (anagen or telogen) and tail skin from litter-matched wt/wt, gt/gt, or flx/flx mice were (**a**, **b**) stained with hematoxylin and eosin or (**c**, **d**) labeled with antibodies to Ki67, (**e**, **f**) desmoplakin, or (**e**, **f**) periplakin. Bars: 100 μm in all panels.

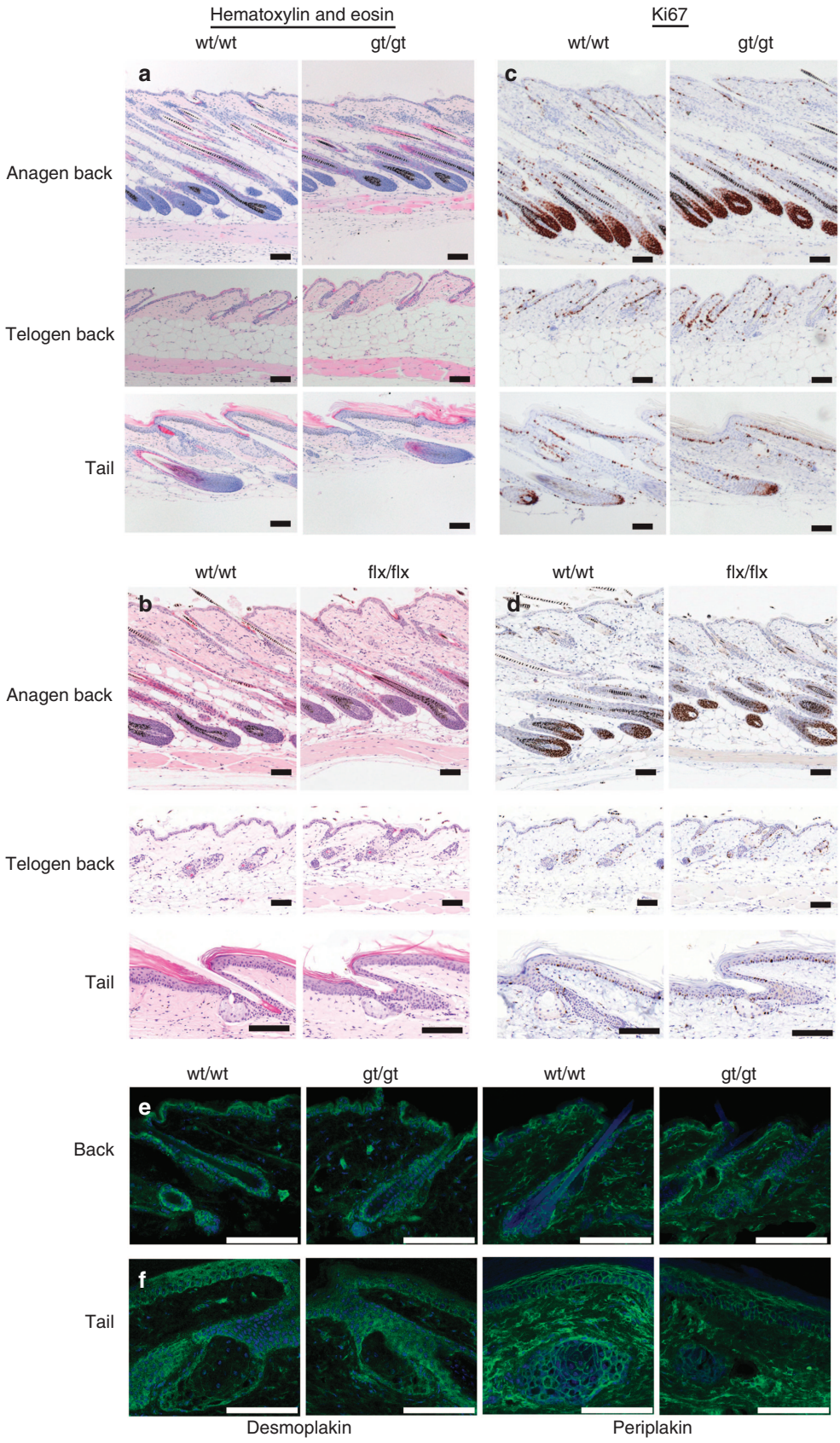
Hematoxylin and eosin
Ki67
wt/wt
gt/gt
wt/wt
gt/gt
a
c
Anagen back
Telogen back
Tail
wt/wt
flx/flx
wt/wt
flx/flx
b
d
Anagen back
Telogen back
Tail
wt/wt
gt/gt
wt/wt
gt/gt
e
Back
f
Tail
Desmoplakin
Periplakin

was overexpressed in cultured human keratinocytes by transient transfection (Figure 3). As reported previously, full-length kazrinA localized to the cytoplasm and, in some cells, also to the nucleus, and caused characteristic changes in cell shape (Figure 3a and b) (Groot *et al.*, 2004; Sevilla *et al.*, 2008a, b). The N-terminal fragment of kazrin, encoded by exons 1–4, did not accumulate in the nucleus, consistent with the lack of an NLS (Figure 3c). Nevertheless, it did cause the same changes in cell shape as full-length kazrinA, with cells forming lamellipodia and filopodia and frequently becoming elongated (Figure 3d and e). The N-terminal coiled-coil domain also accumulated frequently in puncta throughout the cytoplasm (Figure 3e). Almost 60% of cells that overexpressed the N terminus of kazrinA exhibited morphological changes (Figure 3f) ( Sevilla *et al.*, 2008a, b).

We conclude that the ability of kazrin to regulate keratinocyte morphology resides within exons 1–4 of the protein.

**Epidermal phenotype of mice lacking kazrin exons 5–15**

Mice lacking full-length kazrin had grossly normal skin and a normal hair growth cycle (data not shown). H&E-stained sections of the back and tail skin of adult wt/wt, gt/gt, and flx/flx mice did not reveal any differences in overall morphology, irrespective of whether they were examined in telogen or anagen (Figure 4a and b). There were no changes in the cornified layers (Figure 4a and b), and no differences in epidermal proliferation as assessed by Ki67 staining (Figure 4c and d).

As kazrin binds periplakin (Groot *et al.*, 2004) and kazrin overexpression interferes with desmosome assembly (Sevilla *et al.*, 2008a; Nachat *et al.*, 2009), we investigated whether the distribution of periplakin and desmoplakin was affected by the absence of full-length kazrin. We found that expression of desmoplakin and periplakin in both the interfollicular epidermis (IFE) and hair follicles was normal, with both proteins still localizing to cell–cell borders in the epidermis (Figure 4e and f and Supplementary Figure S2 online).

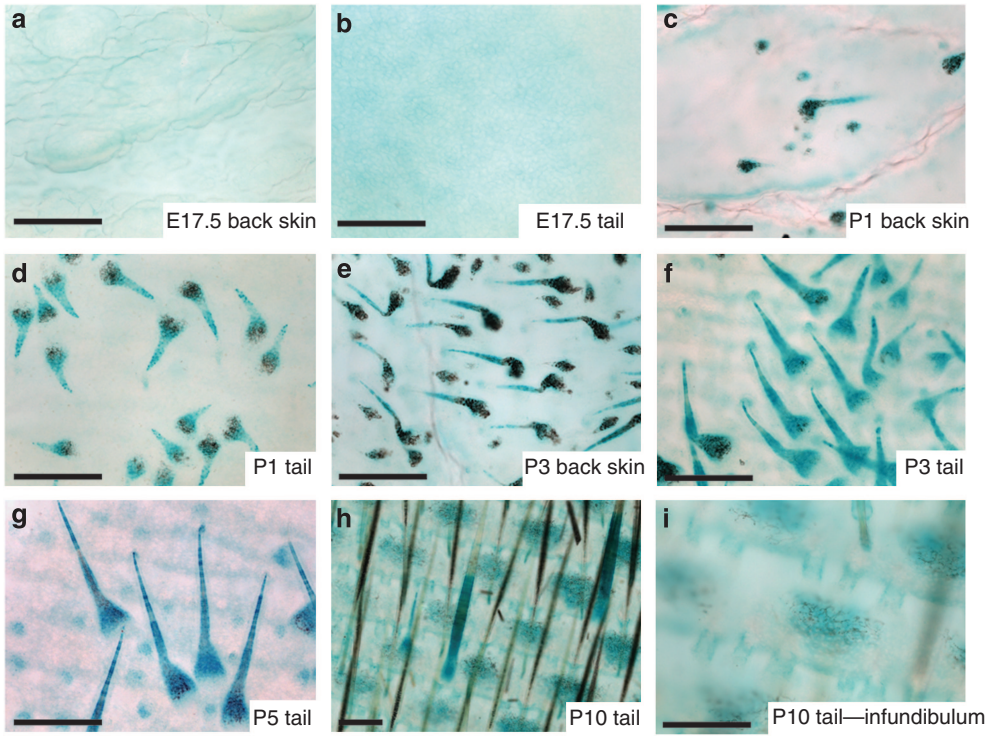


**Figure 5. β-Galactosidase expression in the epidermis of gene-trap mice.** Epidermal whole mounts of back (**a**, **c**, **e**) and tail (**b**, **d**, **f**–**i**) from the ages indicated were stained for X-gal. Bars: 200 μm in all panels. E17.5, embryonic day 17.5; P1, postnatal day 1.

**Figure 6. Kazrin expression in adult mice.** (**a**) Epidermal tail whole mount of kazrin gene-trap (gt/gt) mouse stained for X-gal to visualize endogenous kazrin in hair during anagen. Inf, infundibulum; IRS, inner root sheath. (**b**) Quantitative RT-PCR of mRNA from anagen back skin, telogen back skin, or telogen tail skin using primers to detect all forms of kazrin (exons 6 and 7) or specific for kazrinE (KazE) (exons 10 and 11). The unpaired Student's *t*-test was used to determine whether differences in transcript levels were statistically significant. (**c**–**e**) Paraffin sections of tail-scale interfollicular epidermis from kazrin gt/gt mouse co-stained with antibodies to (**c**, **d**; red) K14 and (**c**, **e**; green) kazrin or (**d**; green) non-immune serum with (blue) 4′,6-diamidino-2-phenylindole (DAPI) nuclear counterstain. Field shown in (**e**) partially overlaps with the field shown in **c**. (**f**, **g**) Frozen section of tail skin from kazrin gt/gt mice stained for (blue) X-gal and counterstained (with nuclear fast red). (**g**) Higher-magnification view of the area demarcated by the black box in **f**. (**h**–**t**) Tail epidermal whole mounts stained with (**h**) non-immune serum, or the antibodies indicated. (**j**) Higher-magnification view of the area demarcated with white dashed line in **i**. (**c**–**e**, **h**–**n**) Blue staining is the DAPI nuclear counterstain. (**j**–**t**) The epidermis from wt/wt mice, except (**l**), which is from gt/gt mouse. Bars: (**a**, **c**, **d**, **f**, **j**–**r**) 100 μm; (**e**) 40 μm; (**h**, **i**) 200 μm; and (**s**, **t**) 50 μm.

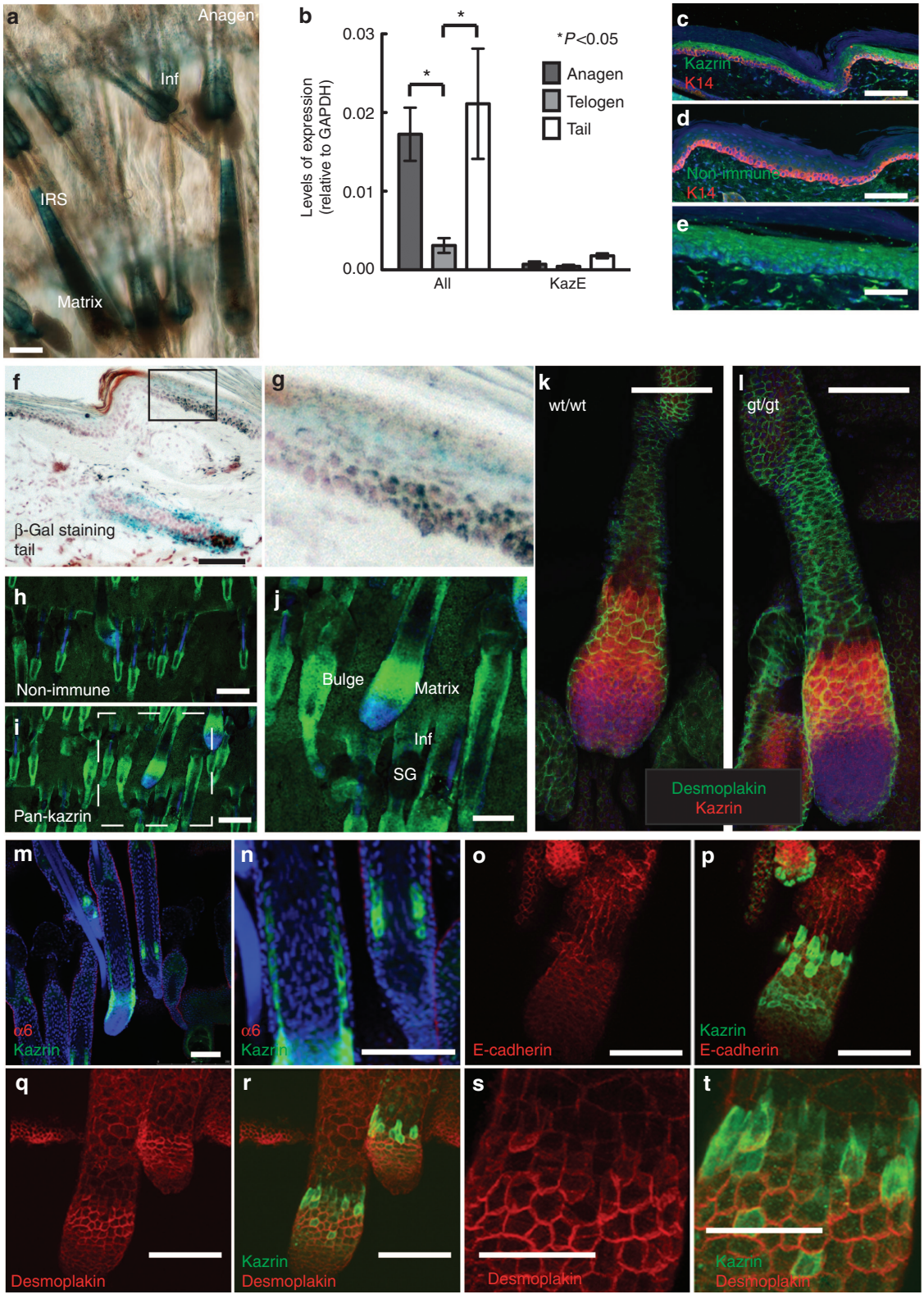
a
Anagen
Inf
IRS
Matrix
b
*P<0.05
Anagen
Telogen
Tail
Levels of expression (relative to GAPDH)
0.03
0.02
0.01
0.00
All
KazE
c
Kazrin
K14
d
Non-immune
K14
e
f
β-Gal staining
tail
g
k
wt/wt
l
gt/gt
Desmoplakin
Kazrin
h
Non-immune
i
Pan-kazrin
j
Bulge
Matrix
Inf
SG
m
α6
Kazrin
n
α6
Kazrin
o
E-cadherin
p
Kazrin
E-cadherin
q
Desmoplakin
r
Kazrin
Desmoplakin
s
Desmoplakin
t
Kazrin
Desmoplakin

**Kazrin expression during epidermal morphogenesis**

We next exploited the gt/gt mice to examine kazrin expression during epidermal morphogenesis. We harvested the epidermis from mice at various developmental stages and performed whole-mount X-gal staining to examine β-galactosidase expression (Figure 5). Kazrin was not expressed in the epidermis before postnatal day 1 (P1) (Figure 5a and b). At P1, β-galactosidase activity was present in developing hair follicles in both back and tail skin (Figure 5c and d). β-galactosidase activity increased in the hair follicles between P1 and P5, as the follicles continued to develop (Figure 5e–g). By P10, when the follicles were synchronously in anagen, β-galactosidase activity was also detectable in the hair follicle infundibulum and in the parakeratotic interfollicular epidermal scales of the tail (Figure 5h and i).

**Kazrin expression in the adult epidermis**

Using whole mounts of tail epidermis, we examined β-galactosidase activity in gt/gt mice at different phases of the adult hair growth cycle (Figure 6a and Supplementary Figure S3 online). β-Galactosidase was detected in the hair follicle infundibulum and IFE of the scales at all stages of the hair cycle and in the bulb of anagen follicles. In addition, we detected kazrin in the inner root sheath at all stages of the hair cycle except for telogen. There was no β-galactosidase activity in the sebaceous glands and non-scale IFE (Figure 6a and Supplementary Figure S3 online).

Levels of endogenous kazrin mRNA in wt/wt mice were measured by quantitative RT-PCR using probes that detected all forms of kazrin or were specific for kazrinE (Figure 6b). As expected from the whole-mount analysis (Figure 6a), levels of kazrin mRNA in the back skin were higher in anagen than in telogen. Kazrin mRNA levels were higher in telogen tail than in anagen back skin, probably reflecting kazrin expression in the interfollicular epidermis of tail but not in back skin. Levels of kazrinE mRNA were considerably lower than levels of total kazrin (Figure 6b), as predicted from the western blots (Figure 2).

To examine kazrin expression at greater resolution, we compared β-galactosidase expression in gt/gt skin with expression of the endogenous protein in wt/wt skin. We stained sections of gt/gt tail skin for β-galactosidase and sections of wt/wt skin with anti-kazrin antiserum (Figure 6c–g). As observed by whole-mount labeling (Figure 5h and i), the expression of β-galactosidase in tail IFE from P10 onward was restricted to the scales, hair follicle bulb, and inner root sheath. This was in good agreement with antibody labeling of tail skin sections (Figure 6c and e). In tail scales, kazrin was weakly expressed in the basal epidermal layer and upregulated in the suprabasal layers (Figure 6c–g).

When whole mounts of wt/wt adult tail epidermis were labeled with the pan-kazrin antibody, the staining pattern was as predicted from the β-galactosidase staining, with labeling of the infundibulum, IFE scale, and anagen bulb (Figure 6h–j). Staining of the hair follicle bulge was non-specific because it was also observed with non-immune serum (Figure 6h). Confocal cross-sections through anagen follicles revealed that kazrin was also expressed in the inner root sheath, again as observed in the reporter mice (Figure 6m and n).

Previous work has shown that overexpression of kazrin results in marked changes in cell shape, with cells becoming elongated (Sevilla *et al.*, 2008a; Figure 3). Co-staining for kazrin and E-cadherin (Figure 6o and p) or desmoplakin (Figure 6q–t) revealed strong expression of kazrin in elongated cells of the upper anagen bulb that exhibited relatively low levels of E-cadherin and desmoplakin. These cells comprise a differentiating population of keratinocytes (Tumbar *et al.*, 2004; Schneider *et al.*, 2009). However, in spite of the inverse correlation between kazrin and desmoplakin in these cells, their number, morphology, and location were unaffected by deletion of kazrin exons 5–15 (Figure 6k and l).

## DISCUSSION

In this report, we have generated two mouse lines, a β-galactosidase gene trap and a conditional knockout, which only express the first four exons of kazrin, and pan-kazrin antibodies to study kazrin expression and function. Using these, we show that in mouse epidermis kazrin has a more restricted distribution than in human and *Xenopus* (Groot *et al.*, 2004; Sevilla *et al.*, 2008a), and that exons 5–15 are dispensable for normal epidermal development and homeostasis. By overexpressing exons 1–4 in cultured keratinocytes, we show that the N terminus and coiled-coil domain of kazrin are responsible for inducing the changes in cell shape observed on overexpression of full-length kazrin (Sevilla *et al.*, 2008a).

In murine epidermis, kazrin expression was first detectable in developing hair follicles at P1. From P10 onward, it was expressed in the bulb of anagen follicles, the infundibulum of all follicles, and in the parakeratotic epidermal scales of the tail. In addition, kazrin was expressed in the inner root sheath of anagen and catagen follicles. We did not detect kazrin in the interfollicular epidermis of mouse back skin. However, in mouse tail, as in human (Groot *et al.*, 2004; Sevilla *et al.*, 2008a) interfollicular epidermis, kazrin expression was upregulated in the differentiating, suprabasal layers of keratinocytes.

Both strains of mice lacking kazrin exons 5–15 were phenotypically normal. Deletion of these exons eliminates translation of the NLS sequence (Figure 2a), and also kazrinE (Nachat *et al.*, 2009). As we confirmed that the region of kazrin encoded by the first four exons does not enter the nucleus (Figure 3c), we conclude that kazrin function is independent of nuclear localization. The lack of any phenotype resulting from the deletion of kazrinE is not surprising given our inability to detect significant levels of endogenous kazrinE mRNA (Figure 6b) or protein (Figure 2e). Although we could detect kazrinE protein in lysates of cultured human keratinocytes, the level was significantly lower than that for the short kazrin isoforms (Figure 2c). We conclude that the C-terminal liprin homology domain of kazrinE, which binds leukocyte common antigen–related and acetylated microtubules, is not required for mouse epidermal development and homeostasis (Sevilla *et al.*, 2008a; Nachat *et al.*, 2009).

There are several potential explanations for the lack of a phenotype in the kazrin gt/gt and flx/flx mice. One is that it reflects the different sites of kazrin expression in the epidermis from different species (humans, *Xenopus*, and mice). Another is that there are compensatory mechanisms that operate in the mouse that are not evident in other species or when cells are placed in culture. This would be surprising, given that kazrin is evolutionarily highly conserved; that the short isoforms have no known homologs that would be obvious candidates for functionally redundant proteins; and that kazrin knockdown in cultured keratinocytes stimulates proliferation and inhibits terminal differentiation (Sevilla *et al.*, 2008a). A third possibility, and one that we favor, given that the expression of exons 1–4 can induce keratinocyte shape changes in culture, is that the functions of kazrin are mediated by the portion of the coiled-coil domain that is encoded by exons 1–4. Coiled-coil domains are well known for their ability to mediate protein–protein interactions (McFarlane *et al.*, 2009), and the kazrin coiled-coil domain binds periplakin (Groot *et al.*, 2004), the p120 subfamily catenin ARVCF, and p190B RhoGAP (Cho *et al.*, 2010). As kazrin lacks any obvious enzymatic function, it is attractive to speculate that its main function is to recruit proteins through the coiled-coil domain. It will therefore be of interest to perform further analysis of kazrin-interacting partners and to delete kazrin exons 1–4 in mice.

## MATERIALS AND METHODS

### Generation of mice lacking exons 5–15 of kazrin

All experiments were carried out under the terms of a UK government Home Office project license, with local ethics approval from the CRUK Cambridge Research Institute. Kazrin β-gal gene-trap reporter mice (gt/gt) were generated from ES cells (clone AN0881; 129SvEv strain) carrying a mutant *Kazrin* locus. ES cells were generated by random insertional mutagenesis with the pGT0lxr-βgeo gene-trap vector containing intronic sequences and a splice acceptor site from the *engrailed-2* gene, the *LacZ* coding sequence, and a neomycin-resistance cassette for selection (Wellcome Trust Sanger Institute Gene Trap Resource, Cambridge, UK). ES cells were injected into C57BL/6 mouse blastocysts to generate germline chimeras. Chimeric mice were mated with F1 mice and offspring heterozygous for the gene-trap insertion ($Kazrin^{+/gt}$) were intercrossed to generate homozygotes ($Kazrin^{gt/gt}$). Mice were maintained in an F1 genetic background (C57BL6/CBA).

As the second strategy to delete kazrin, two conditional knockout ES clones (C57Bl/6N strain) obtained from SIGTR (9030409G11Rik, see SIGTR for construct detail) were injected into eight-cell embryos (CD1). Germline transmission was achieved from both clones by crossing with C57Bl6 females, but long-range PCR and sequence analysis showed that the *LacZ* coding sequence in the gene-targeting cassette contained a deletion in both ES clones. Therefore, we generated a flx/flx mouse. Heterozygous mice derived from one of the two ES clones were mated with 129S4/SvJaeSorGt(ROSA)26Sortm1(FLP1)Dym/JJAX mice (C57BL/6J; Jackson laboratory, Bar Harbor, ME) to remove the FRT-En2-IRES-BGal-loxP-Neo-pA cassette, and then crossed with pGK-Cre-expressing mice (Lallemand *et al.*, 1998) to generate kazrin exon 5–deleted mice ($Kazrin^{wt/flx}$). Mice homozygous for deletion of exon 5 were generated by crossing heterozygous mice and maintained in a C57BL/6J genetic background.

### Kazrin protein purification

Full-length human kazrinA was cloned into the pGEX-6p1 (GE Healthcare, Chalfont St Giles, UK) vector for expression with an N-terminal GST tag and overexpressed in the BL21 (DE3) *E. coli* strain. Transformed cells were grown in LB medium containing 0.1 mg ml$^{-1}$ of ampicillin at 37 °C to an $A_{600}$ of 0.7 (mid-log phase) and induced with 0.1 mM isopropyl-β-D-thiogalactopyranoside at 18 °C for 18 hours. Harvested cells were resuspended in buffer A (2 mM dithiothreitol, 20 mM Tris, pH 7.5, 200 mM NaCl, 5% glycerol) supplemented with EDTA-free protease inhibitors (Roche, West Sussex, UK), 0.6% CHAPs detergent, and 25 U ml$^{-1}$ DNAseI. Cells were lysed by sonication, and the pH of the lysate was adjusted to 7.5. The lysate was clarified by centrifugation at $>100{,}000 \times g$ for 45 minutes. The supernatant was loaded onto a HiTrapQ column followed by a GSTrapHP column (GE Healthcare), both equilibrated in buffer A. The GSTrapHP column was washed with 10 column volumes of buffer A and the GST tag was separated from the kazrinA through on-column digest with PreScission Protease (GE Healthcare) overnight at 4 °C. The tag-less protein was eluted with buffer A and further purified using a 26/60 Sephacryl-200 size-exclusion column (GE Healthcare) equilibrated with buffer A. Fractions containing kazrinA were pooled, concentrated, and stored at −80 °C.

### Generation of pan-kazrin polyclonal antibody

Two rabbits were immunized with full-length human kazrinA using standard techniques (Covalab, Lyon, France). Antibodies in the immune serum and non-immune serum were enriched by purification of the IgG fraction with proteinA sepharose according to the manufacturer's instructions (Thermo Scientific, Hemel Hempstead, Hertfordshire, UK). The different kazrin antisera, termed 943-074 and 943-009, had very similar properties, although 943-074 bound kazrin with slightly higher affinity.

### Cell culture and transient transfection

Mouse keratinocytes were isolated from 7- to 8-week-old dorsal skin and cultured as described previously (Silva-Vargas *et al.*, 2005). Primary human keratinocytes were cultured as described previously (DiColandrea *et al.*, 2000). Cells were transiently transfected with two predesigned, inventoried human kazrin siRNAs, s23404 (5′-AGACUUCAUCCGCAACUAU-3′) and 261163 (5′-CCUGCACAACCCUAUUGU-3′), two mouse kazrin siRNAs (s231975 5′-AGACUUCAUCCGCAACUAU-3′ and s231976 5′-GCACCGCAAGGAGAGUGAA-3′) (Ambion, Applied Biosystems, Paisley, UK), pBb-HA-kazrinA (Sevilla *et al.*, 2008a), or pcDNA3.1/V5/His-kazrin exons 1–4 using the JetPrime Polyfect transfection reagent (PolyPlus Transfection, Nottingham, UK) according to the manufacturer's instructions. Exons 1–4 (amino acids 1–242) of human kazrinA (NP_056024.1) were cloned into pcDNA3.1/V5/His using the TOPO directional cloning kit (Invitrogen, Paisley, UK; catalog no. K4900-01) and the following primers: 5′-CACCATGATGGAAGACAATAAGC-3′ (forward); 5′-CATGGCCAGCTCGGCCTCC-3′ (reverse).

### Immunoblotting and immunoprecipitation

Mouse and human primary cultured cells were lysed in 20 mM Tris, pH 7.4, 150 mM NaCl, 1 mM EGTA, 1 mM EDTA and 1% Triton

X-100. Pan-kazrin polyclonal antibody was crosslinked to ProteinG Dynabeads (Invitrogen) and used to immunoprecipitate kazrin from cleared lysates according to the manufacturer's instructions. Proteins were eluted in standard sample buffer, separated on 4–12% SDS-PAGE gels, and transferred onto nitrocellulose membranes in NuPAGE transfer buffer (Invitrogen) using standard techniques.

Immunoblotting was performed as described previously (Groot *et al.*, 2004). The following antibodies were used (dilutions in brackets): rabbit anti-pan-kazrin (1:500), rabbit anti-peptide antibody to all kazrin isoforms (LS7, 1:500) (Sevilla *et al.*, 2008a), rabbit anti-kazrin (ProteinTech Group, Manchester, UK; 11572-1-AP; 1:500), rabbit pre-immune serum (1:500), mouse anti-α-tubulin (Sigma, Gillingham, Dorset, UK; T6199; 1:2000), and mouse-anti-glyceraldehyde 3-phosphate dehydrogenase (Millipore, Watford, UK; MAB374; 1:500). Fluorescently labeled Li-Cor or horseradish peroxidase-conjugated secondary antibodies were used according to the manufacturer's instructions. Blots labeled with Li-Cor secondary antibodies were imaged using the Li-Cor Odyssey Infrared Imaging System (Li-Cor Biosciences, Cambridge, UK). Horseradish peroxidase -conjugated antibodies were detected using standard ECL reagent (GE Healthcare).

### RT-PCR

RNA was extracted from whole skin or cultured cells using the RNeasy mini kit (Qiagen, Crawley, West Sussex, UK). cDNA was prepared using a Superscript III First-Strand Synthesis Supermix for qRT-PCR kit (Invitrogen) according to the manufacturer's instructions. Quantitative PCR was performed using designed primers with the 7900HT Fast-SyberGreen real-time PCR system (Applied Biosystems). Quantification was based on ΔΔCt calculations, and all samples were compared against mouse glyceraldehyde 3-phosphate dehydrogenase as an endogenous control.

Semiquantitative RT-PCR was performed on DNA from cultured primary mouse keratinocytes with the Fermentas PCR master mix (Fermentas, Thermo Scientific) according to the manufacturer's instructions. The optimal annealing temperature was 55 °C for all the primers, and 35 reaction cycles were performed. PCR reactions were run on 3% agarose gels and detected with SYBR Safe (Invitrogen). Glyceraldehyde 3-phosphate dehydrogenase forward (5′-ACCACAGTCCATGCCATCAC-3′) and reverse (5′-TCCACCACCCTGTTGCTGTA-3′) primers were used. Mouse kazrin primers are listed in Supplementary Table S1 online.

### Immunohistochemistry and epidermal whole-mount labeling

For paraffin sections, tissues were fixed in formal saline and embedded in paraffin wax. For frozen sections, tissues were submerged in OCT compound and frozen on dry ice. Sections—7 μm (paraffin) or 10–12 μm (frozen)—were prepared and collected onto glass slides.

Tail epidermal whole mounts were prepared essentially as described previously (Braun *et al.*, 2003). To separate the epidermis from dermis, skin was incubated at 37 °C in 5 mM EDTA in phosphate-buffered saline (PBS) for 1.5 hours (embryonic to P1 skin) or 4 hours (mice older than P1). The epidermis was fixed in 1% paraformaldehyde for 1 hour at room temperature before labeling with the pan-kazrin antiserum, or in 2% paraformaldehyde for 15 minutes at room temperature before labeling with all other antibodies.

Primary antibodies were used at the following dilutions: Alexa-555-conjugated mouse anti-mouse K14 (1:200), rabbit anti-pan-kazrin (1:100), protein A–purified rabbit pre-immune serum (1:100), rabbit anti-periplakin (TD2, 1:100) (DiColandrea *et al.*, 2000), rabbit anti-desmoplakin (1:200; Santa Cruz Antibodies, Santa Cruz, CA; sc-33555), mouse anti-desmoplakin (115F, 1:50, gift from DR Garrod, University of Manchester, Manchester, UK), rabbit anti-peptide antibody that detects all kazrin isoforms (LS7, 1:50) (Sevilla *et al.*, 2008a), rabbit anti-Ki67 (1:100; Vector Labs, Peterborough, UK; clone SP6, VP-RM04), and mouse anti-V5 (1:500; Invitrogen; R960-25). Species-appropriate secondary antibodies were used to visualize primary antibodies as described previously (Collins and Watt, 2008).

For Ki67 staining, paraffin sections were subjected to antigen retrieval using Ventana CC1 solution under standard conditions (40 minutes, 99 °C) (Ventana Molecular Discovery Systems, Tucson, AZ). Primary antibody was applied for 58 minutes at 37°C. Biotinylated secondary antibody was applied for 30 minutes at 37 °C and visualized using the Ventana DABMap kit according to the manufacturer's instructions. For all other immunohistochemistry of paraffin sections, antigen retrieval was performed by boiling in citrate buffer (pH 6) for 20 minutes. Cultured keratinocytes and frozen sections (thawed briefly) were fixed for 10 minutes in 4% paraformaldehyde at room temperature before labeling, and then permeabilized for 5 minutes with 0.2% Triton X-100 in PBS and blocked with PBS + 10% bovine serum and 3% bovine serum albumin (paraffin sections) or PBS + 0.5% fish skin gelatin, 5% goat serum, and 4% BSA (frozen sections) for 1–2 hours at room temperature. Incubation with primary and secondary antibodies was performed as described previously (Collins and Watt, 2008).

### β-Galactosidase staining

Epidermal whole mounts and frozen sections were fixed in 0.2% glutaraldehyde in 0.1 M phosphate buffer (pH 7.3) supplemented with 2 mM MgCl (PBS-$MgCl_2$) and 5 mM EGTA. Frozen sections were washed twice in PBS-$MgCl_2$ and incubated in PBS-$MgCl_2$ containing 5 mM $K_3Fe(CN)_6$, 5 mM $K_4Fe(CN)_6$, and 1 mM X-gal (5-bromo-4-chloro-3-indolyl β-D-galactopyranoside) overnight at 37 °C to visualize β-galactosidase activity. Fixed epidermal whole mounts were stained similarly, except that washing and staining solutions were supplemented with 0.01% deoxycholate and 0.02% NP-40 (IGEPAL CA-630) to aid permeabilization.

### Image capture

Paraffin sections were imaged using a Zeiss Imager.M2 (Carl Zeiss, Mannheim, Germany). Frozen sections and whole mounts were imaged using a Leica SP5 confocal microscope. For whole mounts, images are presented as maximum projections of a series of Z stacks. Images were optimized for brightness, contrast, and color balance using Adobe Photoshop.

## CONFLICT OF INTEREST

The authors state no conflict of interest.

## ACKNOWLEDGMENTS

This work was supported by Cancer Research UK, the Medical Research Council, the Wellcome Trust, and EU FP7. We gratefully acknowledge the support of Cambridge University and Hutchison Whampoa. Individual authors were supported by the following fellowships: Herchel Smith (MC), FEBS (SC), and the NIH (LS). We thank the core services of the CRUK London

Research Institute, CRUK Cambridge Research Institute, and Wellcome Trust Centre for Stem Cell Research for excellent technical assistance.

## SUPPLEMENTARY MATERIAL

Supplementary material is linked to the online version of the paper at http://www.nature.com/jid

## REFERENCES

Braun KM, Niemann C, Jensen UB *et al.* (2003) Manipulation of stem cell proliferation and lineage commitment: visualisation of label-retaining cells in wholemounts of mouse epidermis. *Development* 130:5241–55

Cho K, Vaught TG, Ji H *et al.* (2010) *Xenopus* kazrin interacts with ARVCF-catenin, spectrin and p190B RhoGAP, and modulates RhoA activity and epithelial integrity. *J Cell Sci* 123:4128–44

Collins CA, Watt FM (2008) Dynamic regulation of retinoic acid-binding proteins in developing, adult and neoplastic skin reveals roles for beta-catenin and Notch signalling. *Dev Biol* 324:55–67

DiColandrea T, Karashima T, Määttä A *et al.* (2000) Subcellular distribution of envoplakin and periplakin: insights into their role as precursors of the epidermal cornified envelope. *J Cell Biol* 151:573–86

Diez-Roux G, Banfi S, Sultan M *et al.* (2011) A high-resolution anatomical atlas of the transcriptome in the mouse embryo. *PLoS Biol* 9:e1000582

Groot KR, Sevilla LM, Nishi K *et al.* (2004) Kazrin, a novel periplakin-interacting protein associated with desmosomes and the keratinocyte plasma membrane. *J Cell Biol* 166:653–9

Kalinin A, Marekov LN, Steinert PM (2001) Assembly of the epidermal cornified cell envelope. *J Cell Sci* 114:3069–70

Lallemand Y, Luria V, Haffner-Krausz R *et al.* (1998) Maternally expressed PGK-Cre transgene as a tool for early and uniform activation of the Cre site-specific recombinase. *Transgenic Res* 7:105–12

McFarlane AA, Orriss GL, Stetefeld J (2009) The use of coiled-coil proteins in drug delivery systems. *Eur J Pharmacol* 625:101–7

Nachat R, Cipolat S, Sevilla LM *et al.* (2009) KazrinE is a desmosome-associated liprin that colocalises with acetylated microtubules. *J Cell Sci* 122:4035–41

Okazaki NRFK, Ohara R, Inamoto S *et al.* (2004) Prediction of the coding sequences of mouse homologues of KIAA gene: IV. The complete nucleotide sequences of 500 mouse KIAA-homologous cDNAs identified by screening of terminal sequences of cDNA clones randomly sampled from size-fractionated libraries. *DNA Res* 11:205–18

Ruhrberg C, Hajibagheri MA, Parry DA *et al.* (1997) Periplakin, a novel component of cornified envelopes and desmosomes that belongs to the plakin family and forms complexes with envoplakin. *J Cell Biol* 139:1835–49

Schneider MR, Schmidt-Ullrich R, Paus R (2009) The hair follicle as a dynamic miniorgan. *Curr Biol* 19:R132–42

Sevilla LM, Nachat R, Groot KR *et al.* (2008a) Kazrin regulates keratinocyte cytoskeletal networks, intercellular junctions and differentiation. *J Cell Sci* 121:3561–9

Sevilla LM, Rana AA, Watt FM *et al.* (2008b) KazrinA is required for axial elongation and epidermal integrity in *Xenopus tropicalis*. *Dev Dyn* 237:1718–25

Silva-Vargas V, Lo Celso C, Giangreco A *et al.* (2005) Beta-catenin and Hedgehog signal strength can specify number and location of hair follicles in adult epidermis without recruitment of bulge stem cells. *Dev Cell* 9:121–31

Tumbar T, Guasch G, Greco V *et al.* (2004) Defining the epithelial stem cell niche in skin. *Science* 303:359–63

Wang Q, Liu M, Li X *et al.* (2009) Kazrin F is involved in apoptosis and interacts with BAX and ARC. *Acta Biochim Biophys Sin (Shanghai)* 41:763–772